Data Mining the OGLE-II I-band Database for Eclipsing Binary Stars

Marco Ciocca
Department of Physics and Astronomy, Eastern Kentucky University, Richmond, KY; marco.ciocca@eku.edu

Presented at the 102nd Spring Meeting of the AAVSO, May 18, 2013. Received April 16, 2013; revised April 26, 2013; accepted April 29, 2013

Abstract The OGLE I-band database is a searchable database of quality photometric data available to the public. During Phase 2 of the experiment, known as "OGLE-II", I-band observations were made over a period of approximately 1,000 days, resulting in over 10^{10} measurements of more than 40 million stars. This was accomplished by using a filter with a passband near the standard Cousins I_c. The database of these observations is fully searchable using the MYSQL database engine, and provides the magnitude measurements and their uncertainties. In this work, a program of data mining the OGLE I-band database was performed, resulting in the discovery of 42 previously unreported eclipsing binaries. Using the software package PERANSO to analyze the light curves obtained from OGLE-II, the eclipsing types, the epochs, and the periods of these eclipsing variables were determined, to one part in 10^6. A preliminary attempt to model the physical parameters of these binaries was also performed, using the BINARY MAKER 3 software.

1. Introduction

The OGLE (Optical Gravitational Lensing Experiment) database contains over 40 million stars, with photometric data accessible to the public. By selecting the number of data points available for a particular star, the quality of the statistics, and the differences between average and median intensity, is possible to extract candidate stars that could be eclipsing binaries. The search was limited to OGLE-II stars (Udalski *et al.* 1997; Szymański 2005) in the Galactic disk (in particular in the constellation Carina) for which the data were reduced using Difference Imaging Analysis (DIA) (Szymański 2005). DIA produces more accurate photometric data, with less uncertainty. Limiting the search to just the Galactic Disk was done in order to generate a smaller sample of stars to analyze. Following the method outlined by Nicholson (2009, 2012), a search of all the data available was initiated with the following MYSQL search parameters:

```
NGOOD>=300 AND NGOOD<=3000 AND I>=13 AND I<=16.5 AND ISIG>=0.05
AND ISIG<=10 AND I>IMED
```

The search parameter constrained the results to stars with at least 300 reliable I-magnitude data points (and less than 3,000), all stars with I-magnitude between 13 and 16.5 and with a standard deviation I_{sig} of the mean I-magnitude between 0.05 and 10. This range of magnitudes was selected to try reducing the overlap with searches of other investigators (Watson *et al.* 2007; Nicholson 2010; Hümmerich 2012; Hümmerich and Bernhard 2012) which had already performed searches on OGLE-II. The upper limit was chosen, on the other hand, to avoid an extremely large number of results. OGLE-II has, in fact, data with mean magnitude I to approximately 22. Had the upper limit for I been so chosen, the returned set would have been in excess of 423,000.

The parameter I_{sig} is the standard deviation of I-magnitude, and therefore it is expected that variable stars will show a value larger than zero, but not so small to just be random noise. The upper extreme was chosen to include all possible cases. Furthermore, as the goal was to search for variable stars of the eclipsing type, stars were selected for which the mean magnitude I was larger than the median I_{med}. This was done because eclipsing variables spend more time at their highest luminosity and dim only during the eclipse, which usually has a duration that is smaller than half of the cycle. This search string netted 285 possible candidates. The same query, but on the Galactic Bulge (OGLE-II had data for that location as well), returns more than 10,000 possible candidates.

2. Data mining results

The candidates were first scrutinized by searching VSX to see if these stars had already been determined to be eclipsing variable or variable in general. This eliminated 77 candidates (Nicholson 2010; Hümmerich 2012; Hümmerich and Bernhard 2012). A smaller number, 25, of the query results were obviously corresponding to stable stars (from inspection of the light curve). These light curves had but one bad data point that created a disparity between I and I_{med} and thus were selected by the MYSQL query. Of the remaining 183, 89 had light curves that did not show an easily recognizable pattern.

To try and visualize the difference between eclipsing variable and other possibly variable stars, we plotted I_{sig} as a function of $(I–I_{med})$. It is expected that stars showing an increase in I_{sig} and also showing an increase of the difference between I and I_{med} would be more likely to be eclipsing variables. The results of such a plot is shown in Figure 1, which clearly shows that stars already identified as eclipsing variables and stars found in this work to be eclipsing variables show a fairly close correlation between I_{sig} and $(I–I_{med})$ (see the R parameters in the linear fit of Figure 1). On the other hand, the 89 stars with no readily recognizable pattern do not show this correlation (R is much smaller). At the end of this analysis, the set of stars to study further was reduced to 94.

We analyzed these data using the software package PERANSO (Vanmuster 2011). This program uses FFT routines to extract, if any, a period of variability

from the light curves obtained from the OGLE-II. In doing this analysis, the end results are phase plots, in which the light curve is folded over a single period showing clearly the eclipsing variability. From the phase plots one can determine the eclipsing types, epochs, and periods of these eclipsing variables. In particular, the results presented in this work were obtained using the routine "Anova" in PERANSO.

The analysis of these 94 candidates found using the MYSQL query is ongoing, and in this paper reports 42 newly identified eclipsing binaries, shown in Table 1. These findings have been submitted to and approved by VSX, managed by the American Association of Variable Stars Observers (AAVSO). Table I reports each star's name, coordinates, eclipsing variable type, period, and magnitude range. The remaining 52 candidates are still in the process of being analyzed and a report on the results will be presented a later date.

Figure 2 (top panel) shows a typical light curve as downloaded from OGLE-II, with the I-band magnitude of the star as a function of the Heliocentric Julian Date (HJD). The period of the star shown in Figure 2 (middle panel) is found to be 0.353095 day. The uncertainty on this period and the periods of all stars in Table 1 are of similar magnitude, approximately 1×10^{-6} d. Such uncertainties arise from the calculation routine itself, as well as the uncertainties of the photometric measurements. In Figure 2 the bottom panel shows the resulting phase plot of the binary star OGLEII CAR-SC2 236.

As is seen from Table 1, eclipsing binaries with the shortest periods are quite often identified as EW eclipsing variables. This designation originates from the star W UMa. The periods for EWs are usually shorter than one day, with the component stars being ellipsoidal in shape due to the gravitational tidal effects on their gas envelopes. EW stars are "over-contact" systems and have light curves that change continuously, so much so that it is almost impossible to specify the exact times of the onset and end of eclipses. The depths of the primary and secondary minima are equal or differ by a small percentage. The component stars generally belong to spectral types F-G. EW eclipsing variables can be described as conjoined twins revolving around each other in a tight pair.

The other types observed are EB and EA. EB (from the prototype β Lyr) are eclipsing systems with ellipsoidal components as well, with the light curves showing continuous changes, as the EW. The difference is that the secondary minimum is always observable, with a depth usually being noticeably smaller than that of the primary minimum; periods also tend to be longer than one day. This property often implies that one star is larger than the other. The components generally belong to spectral types B or A.

Different from the EW and EB types, the EA (from the prototype β Per (Algol)) has components which are mostly spherical. This is because the two stars are farther apart, and the gravitational pull on the gas envelopes is reduced. The beginning and end of the eclipses can be clearly identified in the light

curve. When not in the eclipse the light remains almost constant. EA types have an extremely wide range of periods, from 0.2 day to 10,000 days.

The star displayed in Figure 2 has been identified as an EW eclipsing variable. In Figures 3 and 4 we present two more eclipsing binaries, identified as type EB and EA, respectively.

OGLEII CAR-SC2 47145 has a period of 0.728762 day, while OGLEII CAR-SC3 59302 has a period of 3.022445 days. It should be noted how the simple imagery of the growing component separation from EWs to EBs to EAs is reflected in the period of variability for these three examples. This correlation is reinforced by observing that, in Table I, the periods seem to follow this type-period trend as well.

3. Modeling eclipsing variables

By knowing the period, the light curve shape through the phase plot, and the surface temperature, models reproducing the light curve of the binary systems can be generated. The approach is to match the observed phase plot patterns using well-known parameters of stellar properties (see for example Van Hamme 1993, for tabulated parameters of some of these stellar properties). The surface temperatures and other physical parameters necessary to have a more realistic model of the eclipsing variable identified are not known for the stars in this work, nor are any spectroscopic analyses of these stars known to exist yet in the literature.

The shape of the light curve, however, and the identified eclipsing type permit the construction of plausible models. It is fairly straightforward to match the timing of the eclipses by selecting a suitable mass ratio. The EW star OGLEII CAR-SC2 236 is a classic over-contact system (Robertson and Eggleton 1977): brightness is never constant, with eclipses of similar depth. The measured period is less than 0.4 day and since the system has been identified as a W type, the larger star is likely the cooler star (Bradstreet and Steelman 2004, page 255).

The model of OGLEII CAR-SC2 236 was then built assuming a mass ratio of 3.3 to 1 (the cooler star has a mass 3.3 times the mass of the hotter star) and with temperatures consistent with a G spectral classification. Several parameters in BINARY MAKER 3 can then be input based on this G classification (like limb darkening and reflection parameters). The results of the model are presented in Figure 5.

4. Roche lobes and Lagrangian surfaces

But what exactly is meant by “over-contact? To understand this description let us consider the following: for a single star, the gravitational equipotential lines are concentric spheres. In the case of binary system, the equipotential lines

are still somewhat spherical near the individual stars' centers, but deviate from a spherical shape as one moves away, due to both the influence of the other star's gravitational force and the Coriolis force caused by the rapid rotational motion of the two stars. For each of the two stars in the binary system, the outermost equipotential surface is called the Roche lobe. This surface is elongated and tear-drop shaped, with the long axis along the line joining the two star centers and in contact with the other star lobe precisely at the first Lagrangian point L_1. The L_1 point is where the net force (the sum of the gravitational and centrifugal forces, as a rotating system is non-inertial) is zero. The other point of interest is L_2, still located along a line joining the two stars' centers, but opposite the center of the less massive star. L_2 is where the centrifugal force (again existing because a rotating system is non-inertial) is balanced by the gravitational attraction from the two stars. The gravitational equipotential surface at L_1 is the Inner Critical Lagrangian surface. The one passing through L_2 and encompassing both stars is the outer Lagrangian surface.

As a star in a binary system evolves, it will expand and can fill the inner Lagrangian surface. If material expands beyond this surface, it can cross L_1 and leave the original star and produce mass transfer onto the companion star. Over-contact binaries are those systems where both members have expanded beyond their respective inner Lagrangian surfaces and material is being exchanged. These eclipsing binaries can continue to evolve and possibly join to become a single star.

The model presented in Figure 5 for star OGLEII CAR-SC2 236 shows the fit of the theoretical light curve to the data, the three-dimensional profiles of the two stars, and the outline of the critical equipotential lines. The model predicts that the stars have indeed expanded beyond their inner Lagrangian surfaces. On the outline L_1 (in the center) and L_2 (to the left of the smaller star) are clearly visible. The crosses indicate the star centers and the center of mass of the system. Further, as the eclipses are not total and are continually changing, the angle between the axis of star rotation and the line of sight has to be less than 90 degrees. The angle that gave the best fit to the data was found to be 66.5 degrees.

The model for star OGLEII CAR-SC2 47145 has been built in similar fashion and is shown in Figure 6. This particular system is not quite an over-contact system, but closer to a simpler contact system. The stars appear to have completely filled their inner Lagrangian surfaces but have not expanded beyond them. Systems of this type can be unstable, as the typical star evolution trend is to expand the gas envelope, eventually pushing these binaries to become over-contact systems. In some cases, it is believed that the stars will oscillate between contact and over-contact state (Bradstreet and Steelman 2004, page 241).

As shown in Figure 6, the differences in eclipse depth need to be accounted for. In particular, the flat part of the minor eclipse indicates that one star is

smaller than the other and that the angle between the line of sight and the axis of rotation is close to 90 degrees. The mass ratio that produced the best fit is 0.147 and the surface temperatures were chosen to be 12600 and 11900 K, to be consistent with the fact that EB types are usually B-A stars. The angle between the line of sight and the axis of rotation of this star giving the best fit was found to be 88.2 degrees. A more realistic model could be constructed if data (B–V color terms for example, or spectral analysis or radial velocities) were available that could allow determination of the true surface temperature. Nevertheless, the model and profile in Figure 6 fit the experimental phase plot accurately. The outline and the three-dimensional drawings also show that the hotter star is the more massive one. The Roche lobes for the components are completely filled.

The EA system (OGLEII CAR-SC3 59302) is modeled assuming stars of similar mass and temperature, with a line of sight very close to 90 degrees. The angle that gave the best fit was found to be 86 degrees. The model's results are shown in Figure 7. EA types are clearly of the detached variety, that is, where the stars are still of spherical shape and located well within the inner Lagrangian surface.

Figure 8 shows the model results for OGLEII CAR-SC2 20986. This particular system is complex, as a component of eccentricity had to be added to the orbit of the system to fit the data. Also required was a hot spot on star 1. The eccentricity can be seen by observing the phase plot, where the secondary eclipse is not occurring at phase = 0.5. The hot spot (a location of higher temperature) was needed to account for the shape of the light curve just before the eclipse. The hot spot is visible on the star's three-dimensional profile.

In an elliptical orbit, the Lagrangian inner and outer surfaces change continuously during the orbital period. In Figure 8 we show the shape of the inner Lagrangian surfaces at three points during the orbit: when the stars are at their closest proximity (top panel in Figure 8), at their farthest separation (bottom panel) and at a mid-point of the orbit.

5. Conclusions

By data mining the OGLE I-band database, 42 previously unknown eclipsing variables have been identified. The periods and epochs of these systems have been obtained from their light curves. Based on the shape of the phase plots, models of the binary system studied were constructed which fit the available data. More reliable models could be constructed if the surface temperatures and the radial velocities of the binary components were available.

6. Acknowledgements

This publication makes use of data products from the Two Micron All Sky Survey, which is a joint project of the University of Massachusetts and the

Infrared Processing and Analysis Center/California Institute of Technology, funded by the National Aeronautics and Space Administration and the National Science Foundation.

This research has made use of the VizieR databases operated at the Centre de Données Astronomiques (Strasbourg) in France and of the AAVSO International Variable Star Index (VSX).

The author wishes to thank Dr. Mark Pitts for a careful reading of the manuscript and Dr. J. Cook for securing the purchase of the software BINARY MAKER 3.

References

Bradstreet, D. H., and Steelman, D. P. 2004, BINARY MAKER 3, Contact Software (http://www.binarymaker.com).

Hümmerich, S. 2012, *BAV Rundbrief*, **61**, 10.

Hümmerich, S., and Bernhard, K. 2012, *Perem. Zvezdy, Prilozh.*, **12**, No. 11, 2012.

Nicholson, M. P. 2009, *Open Eur. J. Var. Stars*, **102**, 1.

Nicholson, M. P. 2010, *Open Eur. J. Var. Stars*, **121**, 1.

Nicholson, M. P. 2012, *Discover Your Own Variable Star (New Challenges for Amateur Astronomers*, Amazon Kindle Book (Amazon Standard Identification Number B0074IHO3W).

Robertson, J. A., and Eggleton, P. P. 1977, *Mon. Not. Roy. Astron. Soc.*, **179**, 359.

Szymański, M. K. 2005, *Acta Astron.*, **55**, 43.

Van Hamme, W. 1993, *Astron. J.*, **106**, 2096.

Vanmunster, T. 2011, PERANSO period analysis software (http://www.peranso.com).

Udalski, A., Kubiak, M., and Szymański, M. 1997, *Acta Astron.*, **47**, 319.

Watson, C. L., Henden, A. A., and Price, A. 2007, *J. Amer. Assoc. Var. Star Obs.*, **35**, 414.

Table 1. Eclipsing variables identified and uploaded to the AAVSO International Variable Star Index (VSX).

Name OGLEII CAR-	R. A. h m s	Dec. ° ′ ″	Type	Period (D)	Magnitude Range
SC1 32377	11 05 29.07	–61 13 07.4	EW	0.273914	16.02–16.32 Ic
SC1 51468	11 05 54.64	–61 43 53.9	EW	0.317607	14.50–14.80 Ic
SC1 221876	11 07 02.64	–61 39 43.4	EW	0.351361	15.68–15.90 Ic
SC2 236	11 07 16.05	–61 51 27.8	EW	0.353095	16.34–16.71 Ic
SC1 127704	11 06 20.29	–61 10 05.3	EW	0.377458	16.12–16.40 Ic
SC2 37289	11 07 04.62	–61 06 12.1	EW	0.380999	14.80–15.11 Ic
SC1 162031	11 06 53.95	–61 23 49.0	EW	0.397176	14.89–15.32 Ic
SC3 160527	11 10 25.46	–60 32 04.9	EW	0.399914	16.27–16.50 Ic
SC1 100564	11 06 22.02	–61 39 41.7	EW	0.400404	15.04–15.63 Ic
SC1 172290	11 06 56.03	–61 08 33.3	EW	0.406376	15.83–16.03 Ic
SC1 136161	11 06 19.35	–60 59 50.1	EW	0.420046	15.23–15.43 Ic
SC1 95816	11 06 03.72	–61 46 18.8	EW	0.474436	16.00–16.18 Ic
SC3 134447	11 10 43.60	–61 08 33.5	EW	0.47943	14.54–14.91 Ic
SC3 93572	11 09 55.78	–61 08 20.1	EW	0.48217	15.93–16.13 Ic
SC2 59902	11 07 40.52	–61 32 10.6	EW	0.501492	16.02–16.31 Ic
SC3 11376	11 09 14.83	–61 08 55.0	EW	0.526783	15.45–15.76 Ic
SC3 78518	11 09 32.56	–60 30 21.0	EW	0.547904	13.82–14.10 Ic
SC1 35115	11 05 09.74	–61 08 10.6	EW	0.55131	15.06–15.34 Ic
SC2 62799	11 07 37.75	–61 27 22.6	EB	0.5581	15.68–15.96 Ic
SC1 167381	11 06 37.89	–61 16 05.3	EA	0.664854	14.82–15.33 Ic
SC2 108934	11 08 03.63	–61 17 57.2	EB	0.69084	16.38–16.72 Ic
SC2 47145	11 07 33.92	–61 49 15.9	EB	0.728762	16.34–16.72 Ic
SC3 155559	11 10 47.35	–60 40 38.5	EA	0.875797	15.98–16.37 Ic
SC2 68344	11 07 37.44	–61 21 09.0	EB	1.089216	15.83–16.15 Ic
SC3 59447	11 09 48.73	–61 00 36.0	EA	1.120861	16.3–16.66 Ic
SC3 31284	11 09 04.86	–60 42 20.3	EW	1.162485	14.30–14.50 Ic
SC3 157847	11 10 41.08	–60 37 12.7	EB	1.17131	13.64–14.16 Ic
SC3 83135	11 10 13.57	–61 20 17.3	EA	1.599808	16.29–16.55 Ic
SC2 140728	11 08 37.64	–61 25 44.9	EA	1.705602	14.76–15.4 Ic
SC1 116082	11 06 10.60	–61 24 16.6	EA	1.759605	16.28–16.87 Ic
SC2 20986	11 07 13.93	–61 28 40.5	EA	1.845923	16.33–16.76 Ic
SC1 165151	11 06 43.35	–61 19 58.8	EA	2.384416	16.4–16.9 Ic
SC1 35063	11 05 12.13	–61 07 41.2	EA	2.496182	14.1–14.39 Ic
SC3 93533	11 10 09.60	–61 08 32.3	EA	2.570906	13.2–13.49 Ic
SC3 155588	11 10 37.55	–60 39 24.8	EB	2.763448	15.33–15.56 Ic
SC3 51061	11 09 36.68	–61 11 15.7	EA	2.961514	13.98–14.42 Ic
SC2 158406	11 08 43.38	–61 03 49.6	EA	2.962926	16.22–16.68 Ic
SC3 59302	11 09 39.03	–60 59 18.9	EA	3.022445	14.89–15.31 Ic

Table continued on next page

Table 1. Eclipsing variables identified and uploaded to the AAVSO International Variable Star Index (VSX), cont.

Name *OGLEII CAR-*	*R. A.* *h m s*	*Dec.* *° ′ ″*	*Type*	*Period (D)*	*Magnitude Range*
SC1 151908	11 06 44.52	–61 33 52.9	EA	3.774267	15.57–16.2 Ic
SC3 112892	11 10 05.90	–60 44 01.1	EA	7.014168	16.45–16.79 Ic
SC3 93614	11 10 13.60	–61 06 19.1	EA	7.402731	15.98–16.35 Ic
SC1 51557	11 05 46.20	–61 45 55.7	EA	8.193323	16.43–16.94 Ic

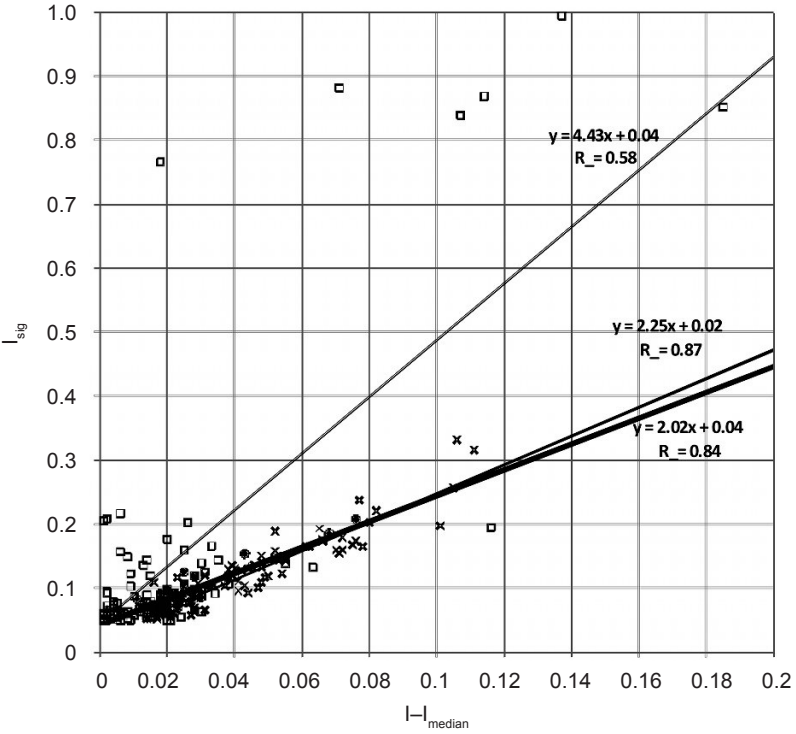

Figure 1. Plot of I_{sig} as a function of ($I–I_{med}$) for stars already identified in the literature as eclipsing variable (medium thickness line), stars identified in this work (thick line), and candidates found with our search parameters and deemed not good candidates for eclipsing variability (thin line). "×" denotes published variables; dots denote this work; open squares denote non-eclipsing.

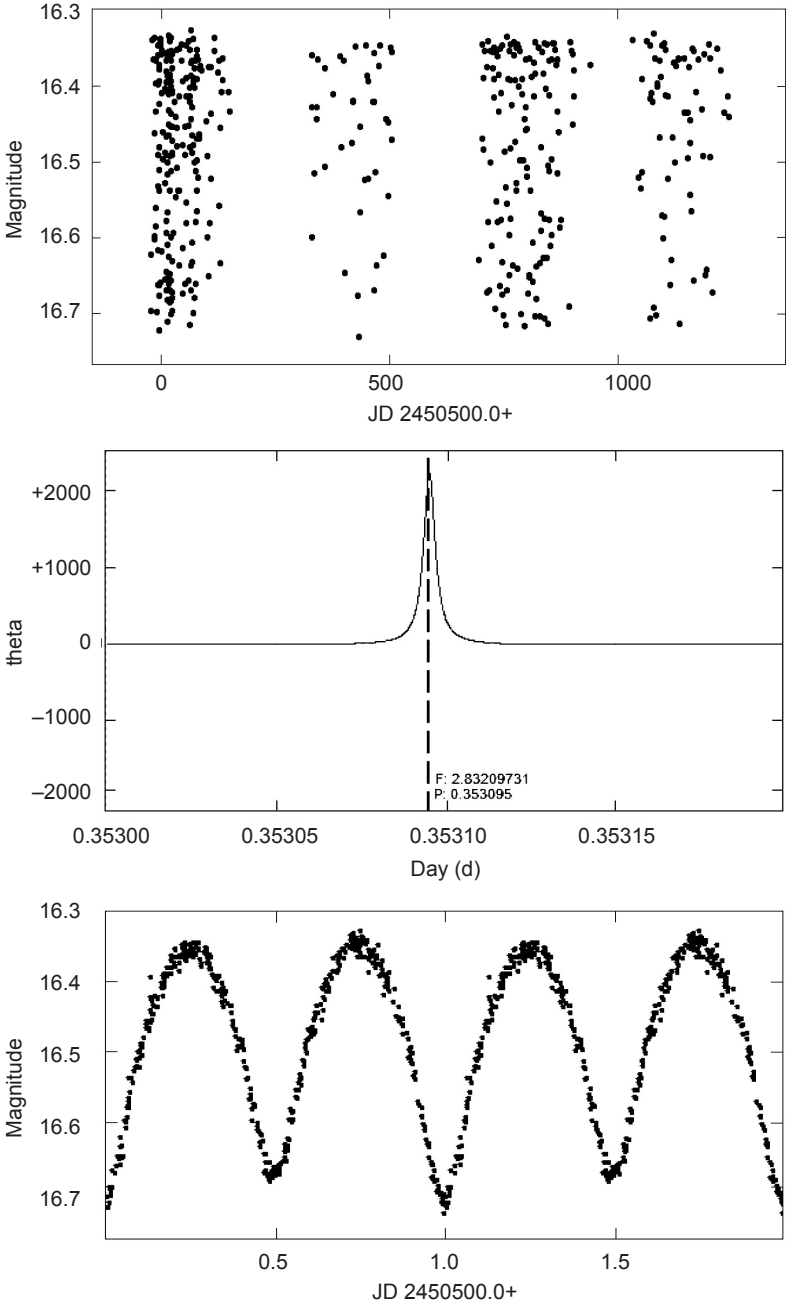

Figure 2. OGLEII CAR-SC2 236. Light curve (top), period (middle), and phase plot (bottom). Type is EW.

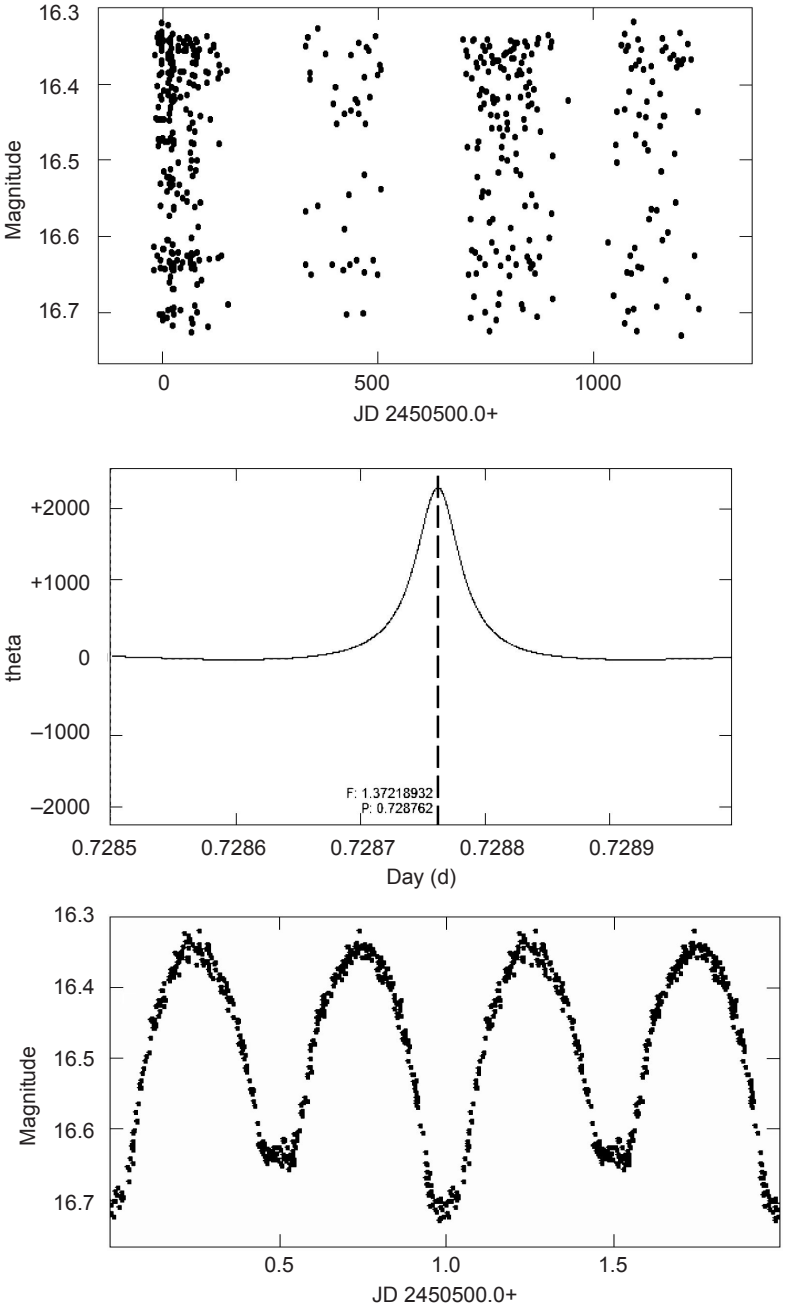

Figure 3. OGLEII CAR-SC2 47145. Light curve (top), period (middle), and phase plot (bottom). Type is EB.

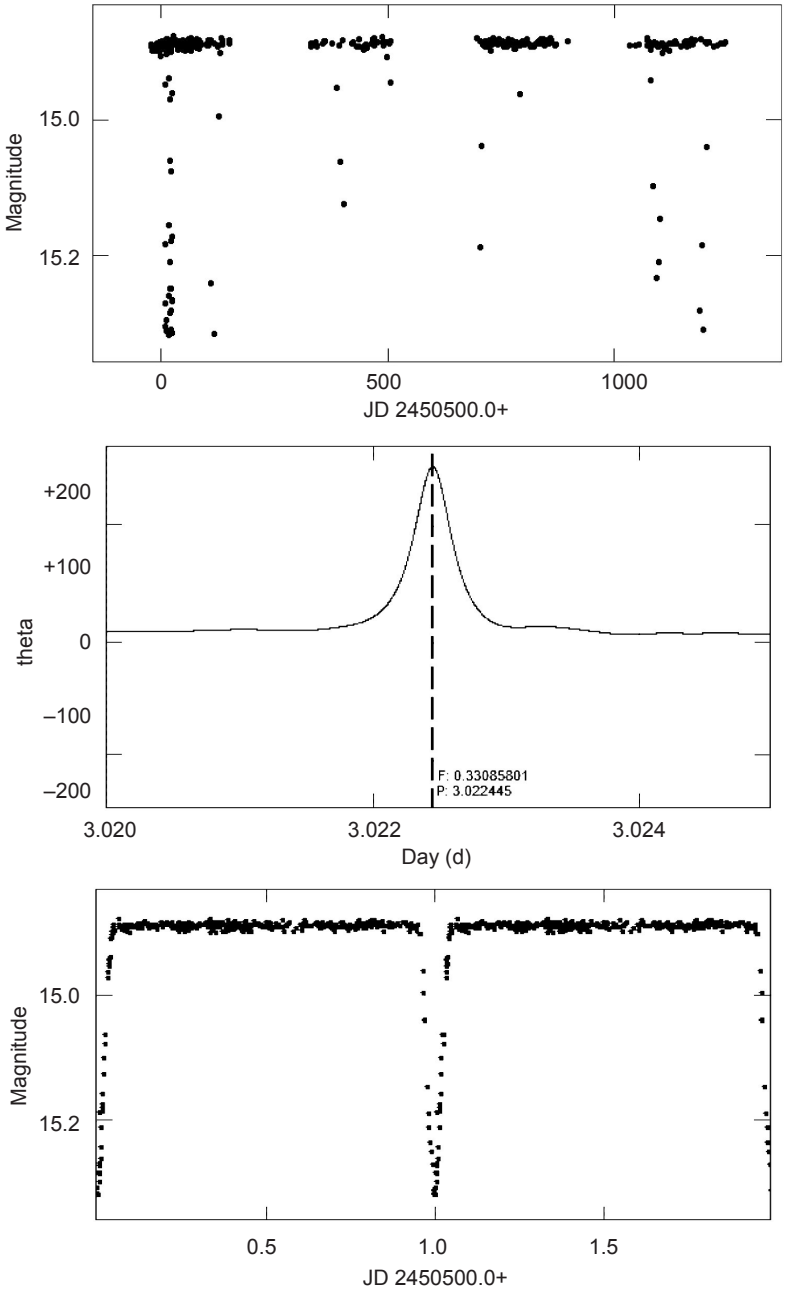

Figure 4. OGLEII CAR-SC3 59302. Light curve (top), period (middle), and phase plot (bottom). Type is EA.

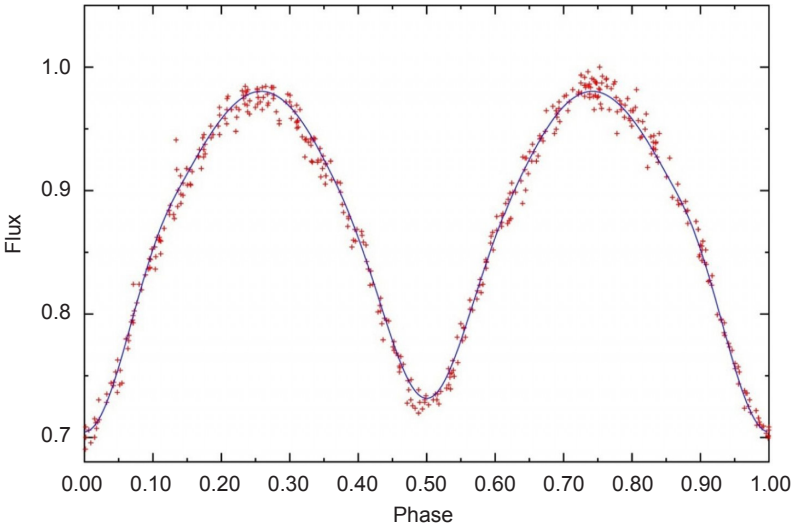

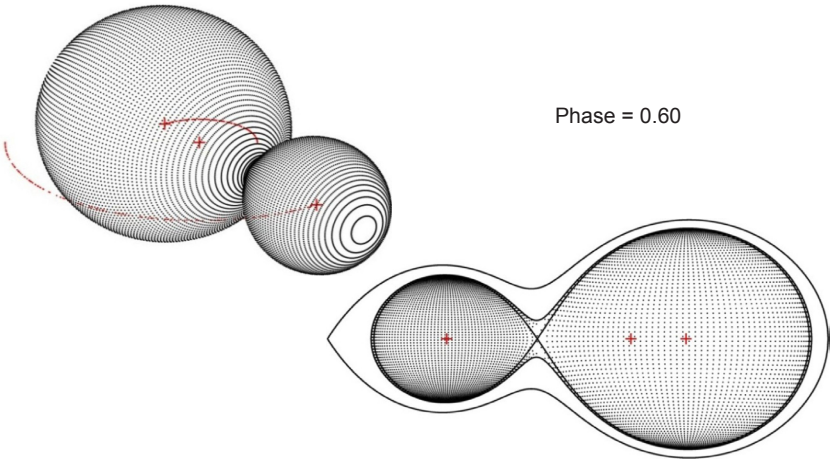

Figure 5. The over-contact binary OGLEII CAR-SC2 236. Phase plot, fit (top), three-dimensional model and equipotential profile (bottom).

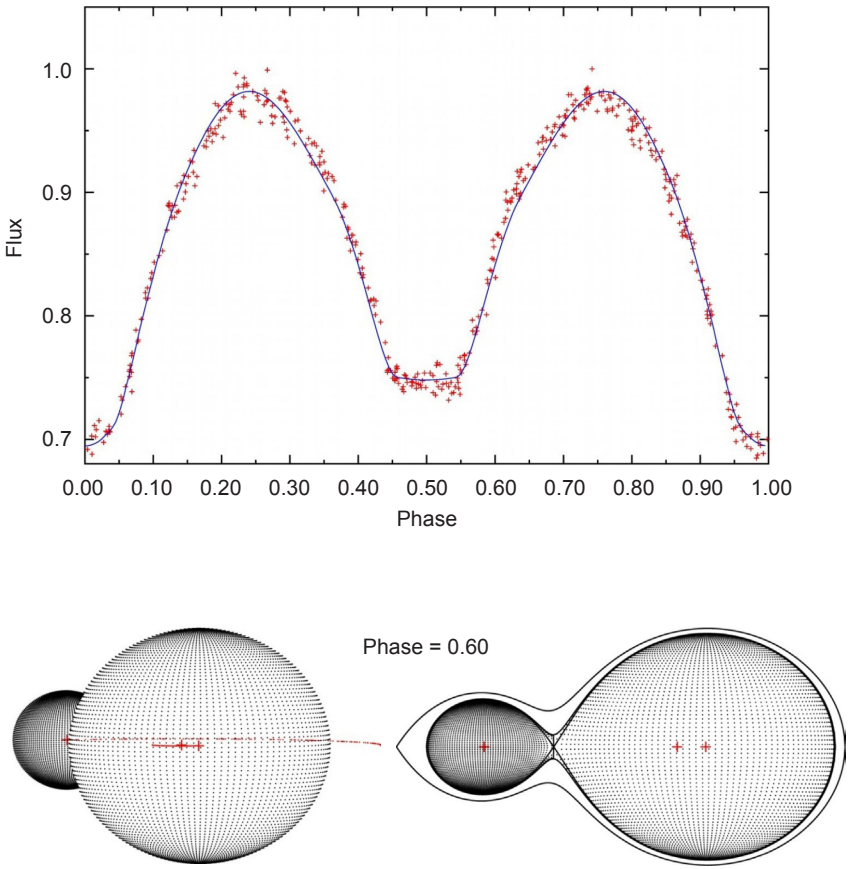

Figure 6. The contact binary OGLEII CAR-SC2 47145. Phase plot, fit (top), three-dimensional model and equipotential profile (bottom).

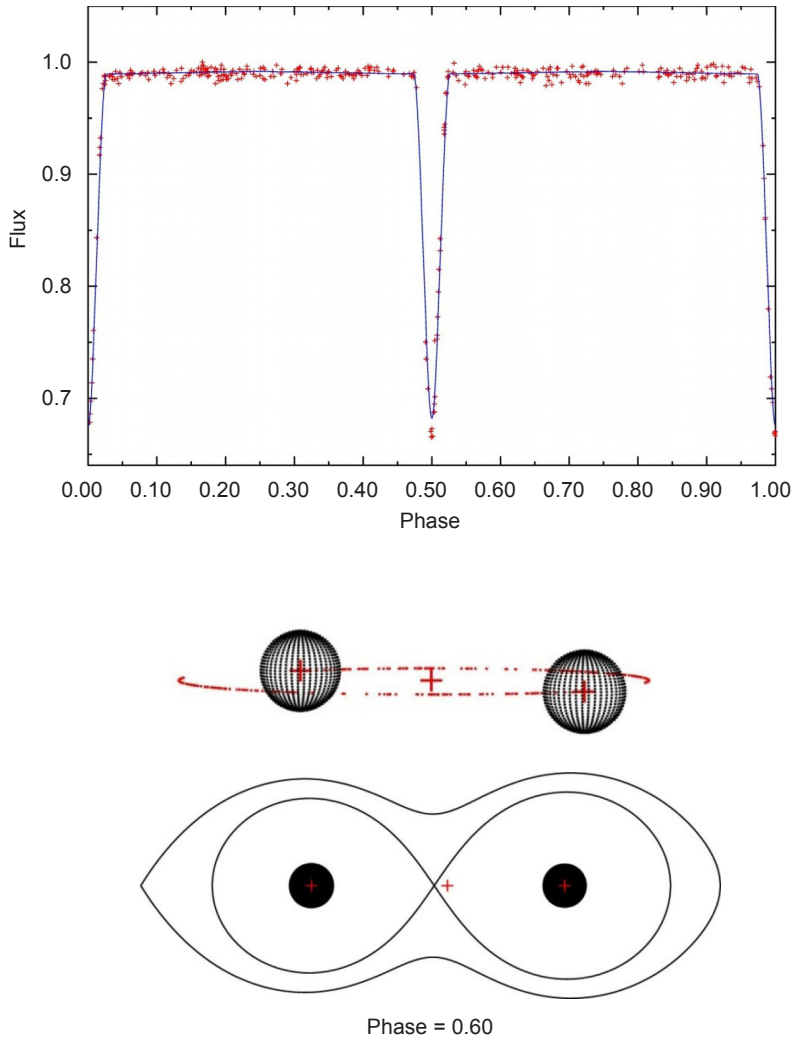

Figure 7. The detached binary OGLEII CAR-SC3 59302. Phase plot, fit (top), and profile (bottom).

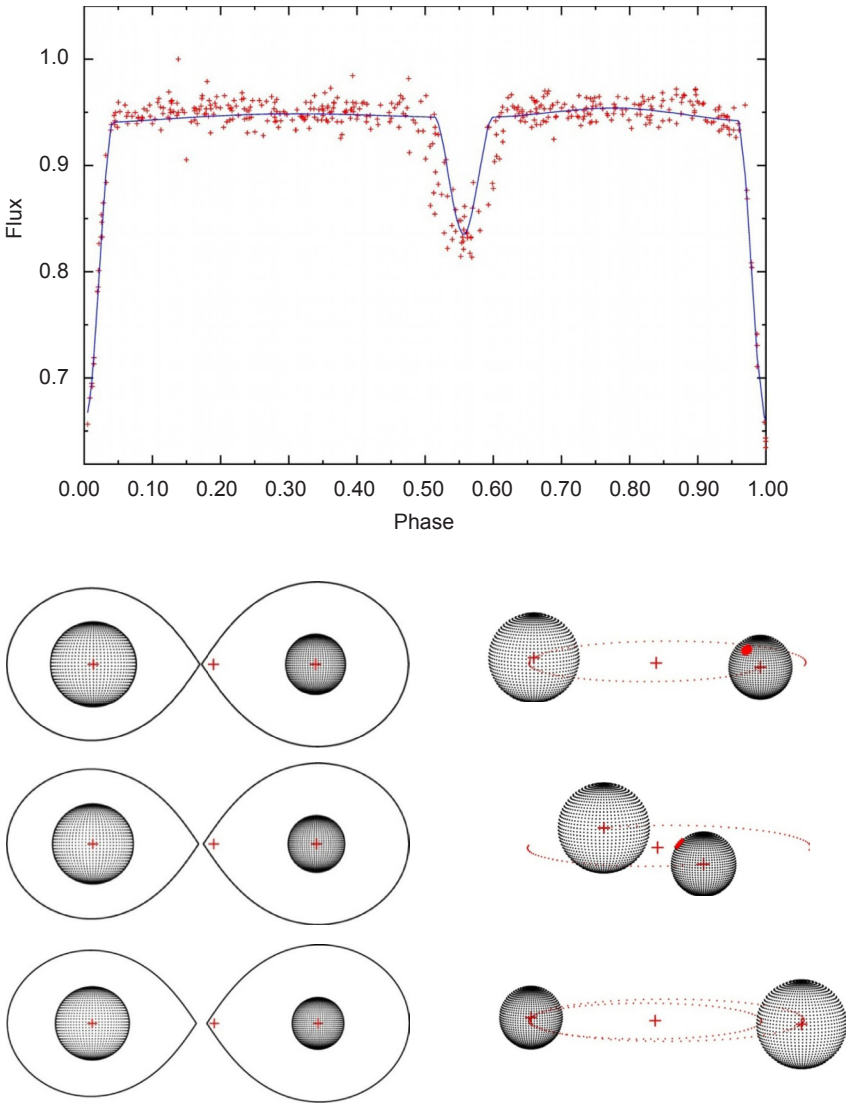

Figure 8. OGLEII CAR-SC2 20986. Phase plot (upper), three-dimensional binary model with corresponding outline (lower). Changing shape of the inner Lagrangian surfaces: at closest proximity (top), at orbital mid-point (middle), and at farthest separation (bottom).